Journal of Statistical Physics, Vol. 48, Nos. 1/2, 1987

Melting of Microinclusions Close Packed in an Elastic Matrix

Eugene V. Kholopov[1]

Received September 11, 1986; revision received February 25, 1987

A novel representation is proposed of the liquid state in a microcavity, the collective nature of that state being taken into account. In this case a microinclusion undergoing melting is described as a single two-level system. The phase transition of melting in a close-packed system of such inclusions embedded in an elastic medium is described rigorously within the framework of the self-consistent approach. When an additional intermediate premelting state is taken into account, the curve of the steady-state phase transition with a critical point that happens on the phase diagram can be transformed in different ways, depending on the values of the specific parameters. In the simplest case shortening of the straight line takes place; bending is also possible. There is a region of the parameters where the critical line is split. In the latter case the existence of the triple point is also possible. The results obtained are in agreement with the experimental data.

KEY WORDS: Thermodynamics; inclusion; melting; phase diagram; critical point; triple point.

1. INTRODUCTION

Compounds with microinclusions are interesting modern materials with respect to their physical properties. In particular, substances in which finely dispersed inclusions of a different material are arranged regularly are of interest at present.[1] The difference of the physical properties of the embedded material gives rise to the fact that every corresponding compound as a whole can manifest itself as a mixture of the constituent components. The effect of melting is typical, with the appropriate melting temperatures of the matrix and the inclusions being different.

[1] Institute of Inorganic Chemistry, Academy of Sciences of the USSR, Siberian Division, 630090 Novosibirsk, USSR.

0022-4715/87/0700-0215$05.00/0

If we restrict ourselves to the case of a matrix with a higher melting temperature, then the process of melting of the embedded particles will be regarded as the partial melting of a solid. Here the observed form of the thermodynamic properties will be dominated by conditions external to the inclusions undergoing the melting. Indeed, if the system involved is free at a given external pressure, then, as is well known, it will exist as a single phase both above and below the melting temperature, i.e., the entire melting process happens just at the melting point. On the other hand, if the volume of our system is fixed, then the vicinity of the phase transition is characterized by the temperature range where both of the phases, liquid and solid, are coexistent.[2] The same behavior, albeit in a significantly narrower temperature interval, seems to be expected when the volume of the material suffering the melting is restricted by elastic external systems. In particular, such a picture must arise for the process of melting sufficiently large inclusions embedded in an elastic matrix, so that the coexistence of the two phases can be realized within every separate inclusion.

In the present paper we consider the opposite limiting situation, when the size of the particles included is negligibly small, so that the coexistence of the two phases within the same particle is impossible. Here the elastic matrix plays the predominant role in two aspects: A temperature range arises where the included particles exist simultaneously, as an ensemble, in both states, solid and liquid. A definite quantitative correlation between the total volumes of those states also takes place. Thus, the partial melting in such a system will manifest itself as a cooperative phenomenon, which, for example, is similar to the melting of sublattices in superionic crystals.[3] Our situation can be regarded as an intermediate case dividing the possibility of the mixture of two different compounds and a homogeneous alloy in the region where it is eutectic.

In the present paper the task of the thermodynamic description of the system of microinclusions has been rigorously solved by means of a modification of the model of Ref. 4. Hence, our system can be regarded as another possible way of realizing an isomorphic phase transition.[5] Despite the model character of the system considered, there is a beautiful example of its experimental realization[6] where the regularly distributed cavities in a zeolite specimen are filled by some metal. The thermodynamic results of the present paper are in agreement with the experimental data.

2. MODEL OF THE STATES OF A MICROINCLUSION

As the model at hand, we consider an elastic matrix containing regularly packed, spherical (for simplicity) cavities of radius R. Atoms filling those cavities are also assumed to have the spherical shape. It is

important that a bulk specimen consisting of such atoms must in general be characterized by a rather high symmetry.[7] Then the solid state of the above system consisting of a few spherically symmetric atoms must naturally be realized as the symmetric configuration of spheres close packed in an admissible cavity as well. Inasmuch as the participation of all the atoms is assumed to be necessary in the process of composing the crystalline state due to the condition that the simultaneous existence of different phases is not admitted in the same cavity, all those identical atoms must stay in equivalent positions. In particular, they must stay same distance from the center of the cavity and therefore belong to one coordination sphere, as shown in Fig. 1a. It is obvious here that the appropriate number n_0 of the atomic positions can be equal to 4, 6, 8, or 12, so that the centers of those atoms are located at the vertices of a tetrahedron, an octahedron, a cube, or an icosahedron, respectively. Note that at least the first three possibilities are natural for cubic crystal symmetry.[7] As far as the molten state is concerned, it must be geometrically stable. On the other hand, it must differ drastically from the crystalline state and be of higher symmetry.

As the simplest realization of the above conditions, the molten state may naturally be described by a configuration where the spherical atoms belong to two coordination spheres so that one of the atoms is located at the center of the cavity, as shown in Fig. 1b. The number n_l of the atomic positions in the liquid state can be calculated as three atoms along the

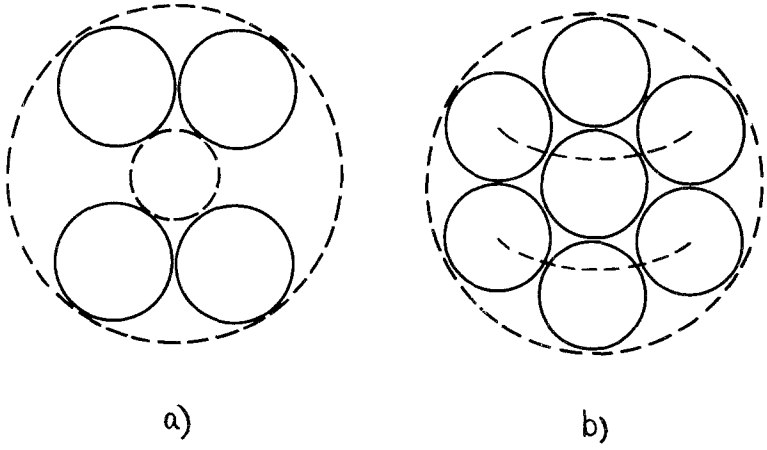

Fig. 1. Central cross section of a spherical cavity of radius R. (a) The case of the solid state for $n_0 = 8$. The cross section is orientated in the plane of two cubic body diagonals. The inner sphere of radius r is plotted by the broken line. (b) The case of the two coordination spheres describing the liquid state. Here $r = a$; the broken curves show the circles that are the loci of the centers of the "side" atomic positions, the length of those circles describing q_l.

polar axis plus the number of atoms that can be arranged along the two independent parallels of latitude, as also shown in Fig. 1b. It is then equal to $n_l = 13.2$. Providing all the atomic positions are occupied in the solid state, the degree of degeneracy of the solid state is equal to $q_0 = 1$, the identity of all the atoms being taken into account. For the liquid state the value of q_l must be calculated taking account of the fact that the atomic position in the center of the cavity must be occupied. As a result, q_l is of the form

$$q_l = \frac{\Gamma(n_l)}{\Gamma(n_l - n_0 + 1)(n_0 - 1)!} \tag{1}$$

where the gamma function $\Gamma(n)$ arises as the result of exhausting all possible atomic arrangements, the relationship $\Gamma(n+1) = n\Gamma(n)$ being used.

Note that the rather large deformation of the constituent atoms happens in the liquid state. Indeed, we assume that the atoms in the solid state are undeformed and fill the cavity without any gap, the configuration of a cube being, for definiteness, realized there. Then the possibility of forming a denser symmetrical configuration such that the same volume of the cavity can contain more atoms may be constructed in such a way that one of the atoms occurs in the center of the cavity inasmuch as this central position is forbidden in the former solid state. The important peculiar feature of the new configuration is its stability even in the case when the number of atoms in the cavity is less than the total number n_l admitted by that configuration. In particular, it is acceptable for the number n_0 of atoms to correspond to the solid state. In the latter case the new configuration may be treated as the excited state of the system of atoms in the cavity. This excited state is characterized by the very high mobility of atoms due to the large number of unoccupied new atomic positions ($n_l > n_0$) and therefore it may be regarded as the liquid state in accordance with the above assumption. The large atomic deformation is the direct geometric consequence of the atomic reconstruction discussed.

Therefore the phase transition between both phases mentioned above seems to be possible only due to the extremely large value of q_l of the corresponding degeneracy ($q_l \gg 1$). The appropriate values of q_l and the outer (R) and inner (r) radii of the coordination sphere in the solid state, which are measured in units of the atomic radius a, for different n_0 are listed in Table I. The obvious condition $r < a$ leads to the conclusion that there is the only admissible coordination sphere. Due to this condition, the given set of magnitudes of n_0 is complete.

The values of the total energy of the atomic states in the cavity can be written in the form

$$E_0 = E_0 + g_0 \Delta V \tag{2}$$

$$E_l = E_l + g_l \Delta V \tag{3}$$

Table I. The Radii R and r Describing the Spherical Cavity[a] and the Degree q_l of Degeneracy of the Liquid State Relative to the Corresponding Solid State for Different Symmetric Arrangements of the Admissible Atomic Positions, Specified by Their Total Number n_0

n_0	4	6	8	12	13.2
$R(+), r(-)$	1.2247 ± 1	1.4142 ± 1	1.7321 ± 1	1.9175 ± 1	2 ± 1
q_l	232.83	879.96	937.69	18.39	1

[a] Expressed in terms of the radius a of the constituent atoms.

Here E_0 and E_l are the values of the energy for a cavity of some definite radius R ($E_0 \ll E_l$), and g_0 and g_l describe the appropriate changes in those energies for a small value ΔV of excess volume of the cavity. The fact that the spherical shape of the cavity is unchanged is the restriction of our model. It is natural to assume that the following inequalities hold:

$$g_l < g_0 < 0 \tag{4}$$

Inasmuch as expressions (2) and (3) determine the energy values of a microscopic object that can exist in two states, depending on its local volume, it is convenient to express the variation of that volume in terms of the strain tensor for the corresponding elastic environment. Here the elastic medium considered is, for simplicity, assumed to be isotropic. On the other hand, it is convenient to describe both states of the microinclusion with the help of the Ising variable $\eta = \pm 1$.

Within the framework of the given model the possibility of some premelting state can also be taken into account. It is obvious that such a state must be distinguished from the ground crystalline state by some additional atomic positions treated as vacancies. Therefore, the above symmetric states with the total number of atomic positions n_j greater than the value of n_0 of the ground state involved can be filled only partly by the constituent atoms and may thus naturally be regarded as premelting ones. It is useful to note at this stage that there may be several states in question. For simplicity, from now on we restrict ourselves to the case of $n_0 = 8$, so that only the intermediate state with $n_1 = 12$ among all the completely symmetric states above may be regarded as the premelting state. Similar to expressions (2) and (3), this state can be described by the parameters E_1 and g_1. The appropriate degree of degeneracy is equal to $q_1 = 495$.

On using the order parameter η, the total energy of the ensemble of atoms in the cavity can be represented in the form

$$E = E_g + J_0\eta + J_1\eta^2 + (t + g\eta)\, u_{\alpha\alpha} \tag{5}$$

where

$$E_g = \frac{\eta_1[E_l(1+\eta_1) - E_0(1-\eta_1)] - 2E_1}{2(1-\eta_1^2)} \tag{6}$$

$$J_0 = \tfrac{1}{2}(E_l - E_0) \tag{7}$$

$$J_1 = \frac{E_l(1+\eta_1) + E_0(1-\eta_1) - 2E_1}{2(1-\eta_1^2)} \tag{8}$$

$$t = \tfrac{1}{2}(g_l + g_0)\, V_0 \tag{9}$$

$$g = \tfrac{1}{2}(g_l - g_0)\, V_0 \tag{10}$$

Here $V_0 = 4\pi R^3/3$ is the volume of the cavity, $u_{\alpha\gamma}$ is the strain tensor at the place where the cavity is located, and summation over repeated tensor indices is supposed. The special form (5) of the expression for the local energy is suitable for what follows. In this case the third intermediate discrete value η_1 of the parameter η is of the form

$$\eta_1 = \frac{2g_1 - g_l - g_0}{g_l - g_0} \tag{11}$$

which is chosen from the condition that after substituting expression (11) into formula (5), the latter must reduce to $E_1 + g_1 \Delta V$.

The extension of the description proposed to the case of several possible premelting states can be realized immediately.

3. THERMODYNAMICS OF A SYSTEM OF MICROINCLUSIONS IN AN ELASTIC MATRIX

Let the above cavities containing the microinclusions form a regular close-packed structure embedded in a uniform and isotropic elastic medium in such a way that direct contacts between different inclusions are absent. The total Hamiltonian consists of two parts: The first is the energy of microinclusions located at the sites of the regular lattice, which are numbered by i and the total number of which N tends to infinity. This part can be expressed as the sum of the terms written in the form (5). The second part is the energy of the elastic matrix. Thus, we have

$$H = H_{\text{inc}} + H_e \tag{12}$$

$$H_{\text{inc}} = \sum_i [E_g + J_0\eta_i + J_1\eta_i^2 + (t + g\eta_i)\, u_{\alpha\alpha}(\mathbf{r}_i)] \tag{13}$$

$$H_e = \int [\lambda/2u_{\alpha\alpha}^2(\mathbf{r}) + \mu u_{\alpha\gamma}^2(\mathbf{r})]\, dV \tag{14}$$

i.e., the deformation originated by the reconstruction in the cavities [formula (13)] is described by the usual quadratic form of the deformational energy.

Here $\mathbf{r}_i$ is the radius vector of the ith cavity; the sum over i is carried out over all the cavities. The expression for H_e is represented in the continuous form,[8] λ and μ are the elastic moduli, $u_{\alpha\gamma}(\mathbf{r})$ is the strain tensor at the point $\mathbf{r}$, and the integration is carried out over the volume V of the matrix containing the lattice of inclusions.

On making use of formula (12), the thermodynamic potential φ of the system at hand can be written in the form

$$\varphi = V\left(\frac{E_g}{v}+\frac{\lambda}{2}\bar{u}_{\alpha\alpha}^2+\mu\bar{u}_{\alpha\gamma}^2+P\bar{u}_{\alpha\alpha}\right)+\varphi_a - T\ln\sum_{\{\eta\}}\left\{\exp\left[-\beta\left(J_0+g\bar{u}_{\alpha\alpha}+\frac{g^2\langle\eta\rangle}{v(\lambda+2\mu)}\right)\sum_i\eta_i - \beta\left(J_1-\frac{g^2}{2v(\lambda+2\mu)}\right)\sum_i\eta_i^2\right]\right\}-\frac{Ng^2\langle\eta\rangle^2}{2v(\lambda+2\mu)} \tag{15}$$

the sequence of the corresponding transformations being described in detail in the Appendix. Here $T=1/\beta$ is the temperature measured in energy units, $v=V/N$, $P=p+t/v$, p is the external pressure, and φ_a is the regular thermodynamic potential of the acoustic phonons; the mean values $\bar{u}_{\alpha\gamma}$ of the strain tensor components are found from the condition that φ be a minimum; and all the terms containing g^2 appear as the result of averaging over the phonon degrees of freedom,[4] the theorem of Ref. 9 being taken into account. In expression (15) the sum over all the configurations of the local order parameters η_i is calculated immediately. On making use of the calculated values of $\bar{u}_{\alpha\gamma}$, expression (15) takes the form

$$\varphi=\varphi_0-\tfrac{1}{2}TN\ln(4q_0q_1)+\tfrac{1}{2}NG\langle\eta\rangle^2-TN\ln(\operatorname{ch}\rho+U) \tag{16}$$

where

$$\varphi_0=N\left(E_g+\frac{D}{1-\eta_1^2}-\frac{vP^2}{2K}\right)+\varphi_a \tag{17}$$

$$K=\lambda+2\mu/3 \tag{18}$$

$$G=\frac{g^2}{v}\left(\frac{1}{K}-\frac{1}{\lambda+2\mu}\right) \tag{19}$$

$$J=\frac{gP}{K}-J_0+G\langle\eta\rangle \tag{20}$$

$$\rho = \beta J + \tfrac{1}{2} \ln(q_1/q_0) \tag{21}$$

$$Q = \frac{q_1}{2(q_0 q_1)^{1/2}} e^{\beta D} \tag{22}$$

$$D = (1 - \eta_1^2)\left(J_1 - \frac{g^2}{2v(\lambda + 2\mu)}\right) \tag{23}$$

$$U = Q \exp(\beta J \eta_1) \tag{24}$$

The mean value $\langle \eta \rangle$ of the order parameter is found by minimizing expression (16), formula (20) being taken into account. As a result, $\langle \eta \rangle$ is determined by a self-consistent equation of the form

$$\langle \eta \rangle = \frac{\operatorname{sh} \rho + \eta_1 U}{\operatorname{ch} \rho + U} \tag{25}$$

The dependences (16)–(25) provide the complete description of the thermodynamics of melting in question.

4. PHASE DIAGRAMS

The self-consistent solution for $\langle \eta \rangle$ that follows from Eq. (25) has the usual character[4] until the right-hand side of Eq. (25) as a function of ρ is specified by the only point of inflection. For simplicity, throughout this paper we restrict ourselves to the condition $\eta_1 = 0$, which corresponds to the symmetric case. Then the phase transition line is straight, as shown in Fig. 2a. The other situation arises when there are three points of inflection in the dependence of the right-hand side of Eq. (25) on ρ. It is important to note here that the splitting of the phase transition occurs when the following inequality is satisfied:

$$D > -0.4655G \tag{26}$$

The corresponding phase diagram is plotted in Fig. 2b. At the critical point the temperature is determined by the equation

$$T_c = \frac{GQ^2}{4(Q^2 - 1)} \tag{27}$$

where the dependence $Q(T)$ at $T = T_c$ is taken into account.

Note that when the internal parameter D is changed out of the region where the two possible phases occur, the parametric condition of the appearance of the splitting of the phase transition describes initially only the immediate vicinity of the critical point in the plane of the external parameters. Therefore, apart from the two critical points, a triple point

must also arise initially on the phase diagram. In the above case of $\eta_1 = 0$ the triple point takes place if both the inequality

$$D < 0.5G \tag{28}$$

and condition (26) are realized simultaneously. The position of the triple point is then specified by the equation

$$\frac{\operatorname{ch} \rho + Q}{1+Q} = \exp \frac{T\rho^2}{2G} \tag{29}$$

The appropriate phase diagram is drawn in Fig. 3.

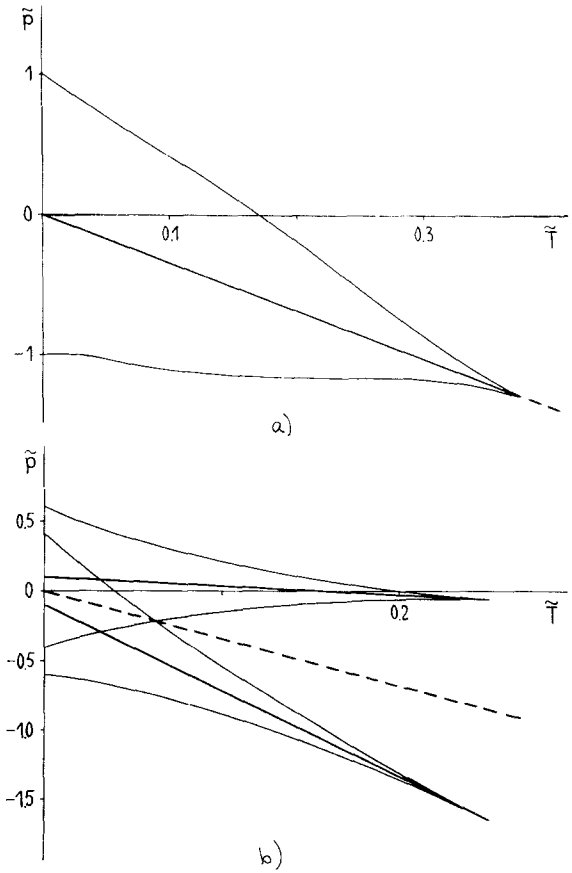

Fig. 2. Phase diagrams represented in the natural axes $\tilde{T} = T/G$, $\tilde{p} = (gP/K - J_0)/G$ at (a) $D/G = -0.6$ or (b) $D/G = 0.6$; $\eta_1 = 0$ in both cases. The steady-state phase transitions and spinodals are depicted by the heavy and thin solid lines, respectively. There are critical points at (a) $\tilde{T} = 0.3775$, $\tilde{p} = -1.2916$ or (b) $\tilde{T} = 0.2500$, $\tilde{p} = -0.0597$ and $\tilde{p} = -1.6514$. The heavy, dashed line terminating at $\tilde{T} = 1$ is the steady-state phase transition line if the intermediate state is absent.

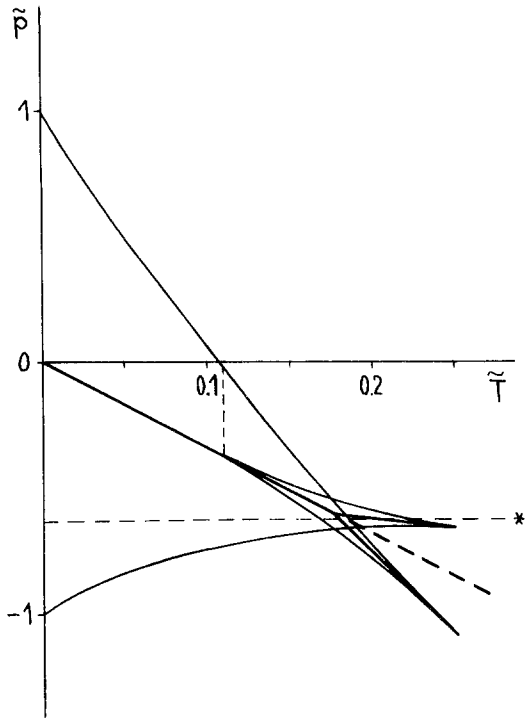

Fig. 3. The pattern of the phase diagram containing the triple point ($\tilde{T}=0.1765$, $\tilde{p}=-0.6038$) and the two critical points ($\tilde{T}=0.2539$, $\tilde{p}=-0.6593$ and $\tilde{p}=-1.0781$) at $D=0$, $\eta_1=0$. The steady-state phase transition curves and spinodals are shown by the heavy and thin lines, respectively. The meaning of the heavy, dashed line is the same as in Fig. 2. The thin broken line points out the position of the point where the spinodals of the intermediate phase terminate ($\tilde{T}=0.1101$). The asterisk labels the path (broken line at $\tilde{p}=-0.63$) along which the heat capacity is drawn in Fig. 4.

The shapes of the boundaries of instability of the metastable phases are determined by the joint solution of Eq. (25) and the expression

$$\Xi \equiv 1-\beta G\frac{1+[(1+\eta_1^2)\operatorname{ch}\rho-2\eta_1\operatorname{sh}\rho]U}{(\operatorname{ch}\rho+U)^2}=0 \tag{30}$$

which is the condition that the total derivative of the right-hand side of Eq. (25) with respect to $\langle\eta\rangle$ is equal to unity, i.e., the spinodals are specified by the points of tangency of both sides of Eq. (25) as functions of $\langle\eta\rangle$.

The corresponding curves are depicted in Figs. 2 and 3 as well. Note that the character of our metastable regions in the vicinity of the triple point (Fig. 3) is qualitatively similar to the case of a first-order phase transition close to a second-order one.[10]

At a fixed pressure the specific heat c_p and the isothermal compressibility $1/K_{is}$ are found upon performing the differentiations in expression (16) and are determined by the formulas:

$$\frac{c_p}{N}=\frac{c_0}{N}+\beta^2 DY[(D+\eta_1 J)\,\mathrm{ch}\,\rho+J\,\mathrm{sh}\,\rho]$$
$$-\beta^2 YZ\left\{\frac{J}{U}+[(1+\eta_1^2)J+\eta_1 D]\,\mathrm{ch}\,\rho-(D+2\eta_1 J)\,\mathrm{sh}\,\rho\right\} \quad (31)$$

$$\frac{1}{K_{is}}=\frac{3V}{4\mu}\left(\frac{\lambda+2\mu}{\Xi K}-1\right) \quad (32)$$

where

$$Y=\frac{U}{(\mathrm{ch}\,\rho+U)^2} \quad (33)$$

$$Z=\frac{\beta DGY(\mathrm{sh}\,\rho-\eta_1\,\mathrm{ch}\,\rho)-J}{\Xi} \quad (34)$$

c_0 is the regular part of the specific heat corresponding to φ_0. The shape of the temperature dependence of the specific heat, which is considered in the region of the split phase transition in the manner pointed out in Fig. 3, is represented in Fig. 4.

The important feature of the solution obtained is its metastable character, associated with the metastability of an intermediate state η_1 relative to both the ground crystalline and the molten states, as is obvious from the discussion of Section 2. Thus, such an intermediate state may arise due to an entropy effect only. Furthermore, a regular description that does not contain the state η_1 also exists and is given by the above formulas with $Q=0$, which coincide with the results of Ref. 4 in the latter case. The corresponding steady-state line of the phase transition can be obtained by continuing the critical straight line in Fig. 2a up to the value of $T/G=1$.

In addition to the formulas given above it is also instructive to obtain the expression for the jump of the enthalpy at the phase transition in the stable case. On the steady-state critical curve the jump of the enthalpy per cavity is as follows:

$$\Delta w = TL(T)\ln(q_{//}/q_0) \quad (35)$$

where the dependence $L(T)$ is specified by the relationship

$$L=\frac{T}{2G}\ln\frac{1+L}{1-L} \quad (36)$$

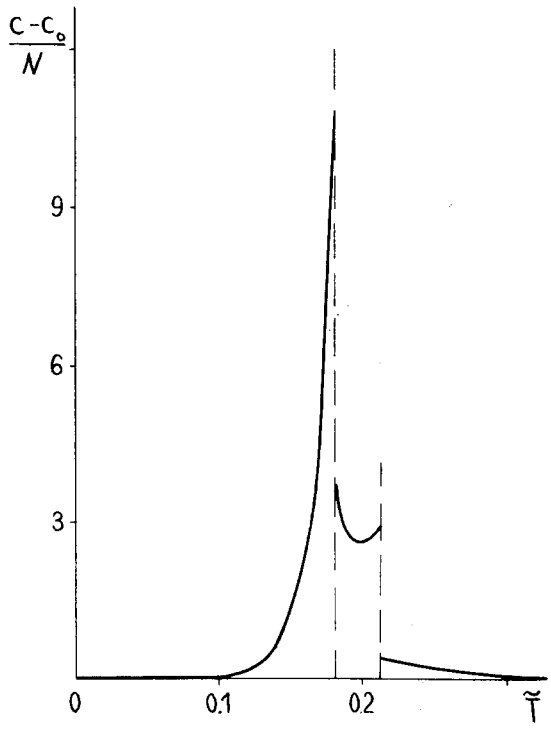

Fig. 4. The heat capacity versus the temperature at $D=0$, $\eta_1=0$, $\tilde{p}=-0.63$. The phase transitions occur at $\tilde{T}=0.1807$ and at $\tilde{T}=0.2130$.

In the case of the intermediate phase the jump of the enthalpy is not determined by a simple formula similar to relationship (35). For its calculation the general expression

$$Nw = N\left[w_0 - \left(J - \frac{G}{2}\langle\eta\rangle\right)\langle\eta\rangle - \frac{DU}{\operatorname{ch}\rho + U}\right] \tag{37}$$

for the enthalpy, which is a direct consequence of formula (16), must be used. Here Nw_0 is the regular contribution corresponding to φ_0.

Now we compare the results of the present paper with the experimental data for the melting of cubic clusters consisting of eight atoms of metallic indium occupying the cavities of a zeolite matrix.[6] The structure of those clusters enables us to employ directly the obtained formulas for the case of the only intermediate state. Putting $T_c=243$ K, $\Delta w \approx 41.6\times10^{-16}$ erg/cavity in the case of $\eta_1=0$, and we see that the phase transition takes place in the vicinity of the critical point. Moreover, splitting of the phase transition can also occur with the corresponding

estimates $G \approx 730$ K and $D \lessapprox -340$ K not being in contradiction with our model representations, but the temperature range of splitting is very small there.

5. CONCLUSION

The present results may be divided into two parts. First, based on the available experimental data, an attempt has been made to describe the model states specifying an idealized microinclusion in the process of melting. Despite the phenomenological character of the construction, the latter seems to be the reasonable origin, allowing us to obtain the prediction of the abnormally large statistical factors accompanying the process of melting, so that the phenomenon of melting may be treated as essentially local. As a result, the dependence of the states of a single microinclusion on the external parameters, which arises naturally in our consideration, enables us to describe those states with the help of a scalar order parameter.

The other results are connected with the investigation of the different possible types of phase diagram, depending on the parameters of the system. In the considered case of only one intermediate state, this state is the predominant one in some phase. However, the situation can arise that the appropriate phase is unstable and does not arise on the phase diagram. Then the phase diagram has a single critical line terminating at the critical point. This critical line is straight when $\eta_1 = 0$; otherwise it is curved. The stabilization of the intermediate phase gives rise to the splitting of the phase transition, so that a triple point can exist. The obvious extension of this result to the case of several intermediate states, which is also the most typical case for the phenomenon of melting, is the prediction of the multiple splitting of the phase transition, which happens in the ensemble of the corresponding microscopic systems embedded into the elastic medium. Note that taking account of additional intermediate states, which are metastable on the microscopic level, gives rise to a significant increase in the pressure of the critical point where the phase transition line terminates. This tendency can promote the possibility of observing experimentally the critical points in the solid system described. Note also that the prediction of the critical points does not contradict the process of melting for the systems involved inasmuch as the crystallization of microinclusions is not connected with the creation of any long-range order in the crystallographic sense; the local mechanisms that give rise to a definite orientation of the solid cluster above are dropped here because they do not change the main results.

In conclusion we note that an important feature of the present approach is as follows: On one hand, the model in question can be calculated quite accurately. On the other hand, this model is very realistic, so that its direct practical realization is possible, as mentioned above.

At this stage of discussion the following question arises: What is the field of application of the model? Is this restricted only to physical problems in the narrow class of special materials? We believe that the results give general grounds on which to understand many cooperative phenomena in heterostructures.

APPENDIX

All the calculations here are carried out following Ref. 4. The quantities η_i and $u_{\alpha\gamma}(\mathbf{r})$ may be expressed in terms of their Fourier transforms by the formulas

$$\eta(\mathbf{r}) = \frac{1}{V^{1/2}} \sum_{\mathbf{k}} \eta_{\mathbf{k}} \exp(i\mathbf{kr}) \tag{A1}$$

$$u_{\alpha\gamma}(\mathbf{r}) = \bar{u}_{\alpha\gamma} + \frac{i}{2V^{1/2}} \sum_{\mathbf{k}}{}' (k_\alpha u_\gamma^{\mathbf{k}} + k_\gamma u_\alpha^{\mathbf{k}}) \exp(i\mathbf{kr}) \tag{A2}$$

Here the density $\eta(\mathbf{r})$ is connected with the local quantity η_i by the relationship $\eta(\mathbf{r}) = \eta_i/v$ for every vector $\mathbf{r}$ terminating in the ith unit cell, v is the volume of the unit cell, $\bar{u}_{\alpha\gamma}$ is the mean value of the strain tensor, and $\mathbf{u}^{\mathbf{k}}$ is the Fourier transform of the displacement vector; the prime on the summation sign indicates that the term with $\mathbf{k} = 0$ is omitted.[11] Indeed, there is no phonon corresponding precisely to $\mathbf{k} = 0$. Strictly speaking, the summation in expression (A2) is carried out over a denumerable set of values of $\mathbf{k}$, whereas the sum in expression (A1) is over the lowest N values of $\mathbf{k}$ of the same set (this is accomplished by a suitable choice of the boundary conditions). However, within the statistical accuracy, the difference between the above regions of summation may be ignored.

The thermodynamic potential φ is of the form

$$\varphi = -T \ln \mathrm{Tr}[\exp(-\beta H - \beta V p \bar{u}_{\alpha\alpha})] \tag{A3}$$

where $T = 1/\beta$ is the temperature in energy units, p is the external pressure, and H is specified by formula (12); the trace is over all the configurations at hand. On substituting formulas (A1) and (A2) into expressions (13) and (14), we can rewrite formula (A3) in the form

$$\varphi = V\left(\frac{E_g}{v} + \frac{\lambda}{2}\bar{u}_{\alpha\alpha}^2 + \mu\bar{u}_{\alpha\gamma}^2 + P\bar{u}_{\alpha\alpha}\right) + \varphi_a$$
$$- T \ln \mathrm{Tr}\left\{\left\langle \exp\left[-\beta(J_0 + g\bar{u}_{\alpha\alpha})\sum_i \eta_i\right.\right.$$
$$\left.\left. - \beta J_1 \sum_i \eta_i^2 - i\beta g \sum_{\mathbf{k}}{}' (\mathbf{ku}^{\mathbf{k}})\,\eta_{-\mathbf{k}}\right]\right\rangle_a\Bigg\} \tag{A4}$$

Here $P = p + t/v$, and the formal procedure of separating the contribution of the noninteracting phonons[12] is carried out within the statistical accuracy. Here

$$\varphi_a = -T \ln \mathrm{Tr}[\exp(-\beta H_a)] \tag{A5}$$

$$H_a = \frac{\lambda + 2\mu}{2}\sum_{\mathbf{k}}{}' |(\mathbf{ku}^{\mathbf{k}})|^2$$
$$+ \frac{\mu}{2}\sum_{\mathbf{k}}{}' (k^2 |\mathbf{u}^{\mathbf{k}}|^2 - |(\mathbf{ku}^{\mathbf{k}})|^2) \tag{A6}$$

H_a corresponds to Hamiltonian (14). As a result, the trace in formula (A4) is only over the configurations of η_i, whereas $\langle \cdots \rangle_a$ denotes the average over the phonons described by the Hamiltonian (A6).

Due to the parabolic form of the Hamiltonian (A6), after averaging, the exponential in expression (A4) takes the form

$$\exp\left[-\beta(J_0 + g\bar{u}_{\alpha\alpha})\sum_i \eta_i - \beta J_1 \sum_i \eta_i^2 + \frac{\beta g^2}{2(\lambda + 2\mu)}\sum_{\mathbf{k}}{}' |\eta_{\mathbf{k}}|^2\right] \tag{A7}$$

The last term in the square brackets in expression (A7) may be transformed by adding and submitting the appropriate term with $\mathbf{k} = 0$ into the form

$$\frac{\beta g^2}{2v(\lambda + 2\mu)}\left[\sum_i \eta_i^2 - \frac{1}{N}\left(\sum_i \eta_i\right)^2\right] \tag{A8}$$

For the further transformation of the trace in formula (A4), where expressions (A7) and (A8) are taken into account, it is useful to apply the following statistical identity[9]:

$$\mathrm{Tr}\left\{\exp\left[NL\left(\frac{1}{N}\sum_i \xi_{1i}, \ldots, \frac{1}{N}\sum_i \xi_{ni}\right)\right]\right\}$$
$$= \exp\left[NL(\langle\xi_1\rangle, \ldots, \langle\xi_n\rangle) - N\sum_j \frac{\partial L(\langle\xi_1\rangle, \ldots, \langle\xi_n\rangle)}{\partial\langle\xi_j\rangle}\langle\xi_j\rangle\right]$$
$$\times \mathrm{Tr}\left\{\exp\left[\sum_j \frac{\partial L(\langle\xi_1\rangle, \ldots, \langle\xi_n\rangle)}{\partial\langle\xi_j\rangle}\sum_i \xi_{ji}\right]\right\} \tag{A9}$$

where L is a differentiable function of n variables, and $j = 1,..., n$ labels the physical quantities of interest. In our case $n = 2$, $\xi_{1i} = \eta_i$, $\xi_{2i} = \eta_i^2$, and the trace above converts into the form

$$\exp \frac{N\beta g^2 \langle \eta \rangle^2}{2v(\lambda + 2\mu)} \operatorname{Tr} \left\{ \exp \left[-\beta \left(J_0 + g\bar{u}_{\alpha\alpha} + \frac{g^2}{v(\lambda + 2\mu)} \right) \right. \right.$$
$$\left. \left. \times \sum_i \eta_i - \beta \left(J_1 - \frac{g^2}{2v(\lambda + 2\mu)} \right) \sum_i \eta_i^2 \right] \right\} \tag{A10}$$

On replacing the trace in formula (A4) with expression (A10), we readily obtain formula (15) of interest. So the molecular field arises as a rigorous physical field.

Note that the effect involved is the manifestation of a long-wavelength acoustic anomaly, which is described correctly by the Hamiltonian (A6). On the other hand, the corresponding spectrum is, strictly speaking, the long-wavelength part of the real spectrum. However, the corrections corresponding to the appropriate deviation of the real short-wavelength part of the spectrum from its linear extrapolation are rather small.[13]

ACKNOWLEDGMENTS

I am grateful to Prof. V. N. Bogomolov for his attention and encouragement and also to Prof. A. R. Regel and the participants of the seminar headed by Prof. V. N. Bogomolov for helpful discussions.

REFERENCES

1. D. J. Bergman, *Phys. Rep.* **43**:377 (1978).
2. L. D. Landau and E. M. Lifshitz, *Statistical Physics* (Nauka, Moscow, 1976).
3. V. R. Belosludov, R. I. Efremova, and E. V. Matizen, *Fiz. Tverd. Tela* **16**:1311 (1974); *Sov. Phys. Solid State* **16**:847 (1974).
4. E. V. Kholopov, *Zh. Eksp. Teor. Fiz.* 77:293 (1979) [*Sov. Phys. JETP* **50**:151 (1979)].
5. V. L. Pokrovskii and G. V. Uimin, *Zh. Eksp. Teor. Fiz.* **55**:1555 (1968).
6. Yu. A. Alekseev, V. N. Bogomolov, V. A. Egorov, V. P. Petranovskii, and S. V. Kholodkevich, *Pis'ma Zh. Eksp. Teor. Fiz.* **36**:384 (1982) [*Sov. Phys. JETP Lett.* **36**:463 (1982)].
7. C. Kittel, *Introduction to Solid State Physics* (Wiley, New York, 1971).
8. L. D. Landau and E. M. Lifshitz, *Theory of Elasticity* (Nauka, Moscow, 1965).
9. E. V. Kholopov, *Phys. Lett.* **73A**:377 (1979).
10. E. V. Kholopov, *Fiz. Tverd. Tela* **21**:2814 (1979) [*Sov. Phys. Solid State* **21**:1620 (1979)].
11. A. I. Larkin and S. A. Pikin, *Zh. Eksp. Teor. Fiz.* **56**:1664 (1969); *Sov. Phys. JETP* **29**:891 (1969).
12. V. M. Nabutovskii and E. V. Kholopov, *Teor. Mat. Fiz.* **26**:376 (1976).
13. E. V. Kholopov, *Phys. Lett.* **79A**:464 (1980).